Modeling and measurement of losses in silicon-on-insulator resonators and bends

Shijun Xiao, Maroof H. Khan, Hao Shen and Minghao Qi

Birck Nanotechnology Center, Purdue University, West Lafayette, IN 47907, USA
sxiao@ecn.purdue.edu, mhkhan@purdue.edu, shen17@purdue.edu, mqi@ecn.purdue.edu

Abstract – We present an analytical model to quantify losses in resonators and bends without uncertain contributions from fiber coupling in/out or waveguide cleavage facets. With resonators in add-drop configuration, intrinsic losses are calculated from the free spectral range, through-port extinction and drop-port bandwidth. We fabricated and characterized silicon-on-insulator resonator for loss analysis. At 1.55 μm, racetrack resonators with a bending radius of 4.5 μm show intrinsic losses as small as 0.14±0.014 dB/round-trip. Meanwhile, intrinsic losses increase up to 1.23 dB/round-trip in the racetrack resonator that has a bending radius of 2.25 μm. Losses in a 180° bend are estimated as a half of the intrinsic losses in these racetrack resonators, *i.e.*, 0.07±0.007 dB/turn for a bending radius of 4.5 μm and 0.62 dB/turn for a bending radius of 2.25 μm. Loss in a 90° bend with a radius of 4.5 μm is determined to be 0.06±0.006 dB/turn at 1.55 μm. The losses in 180° or 90° bends are found to be mainly due to the transition loss between waveguide bends and straight waveguides.

OCIS codes: 250.5300 (photonic integrated circuits); 130.3120 (integrated optical devices); 230.5750 (resonators); 220.4000 (microstructure fabrication)

References and Links

1. K. K. Lee, D. R. Lim, H.C. Luan, A. Agarwal, J. Foresi, and L. C. Kimerling, "Effect of size and roughness on light transmission in a Si/SiO2 waveguide: experiments and model," Appl. Phys. Lett. **77**, 1617 (2000).
2. K. K. Lee, D. R. Lim, and L. C. Kimerling, "Fabrication of ultralow-loss Si/SiO2 waveguides by roughness reduction," Opt. Lett. **26**, 1888-1890, (2001).
3. Y. Vlasov and S. McNab, "Losses in single-mode silicon-on-insulator strip waveguides and bends," Opt. Express **12**, 1622-1631 (2004).
4. J. Niehusmann, A. Vörckel, P. H. Bolivar, T. Wahlbrink, W. Henschel and H. Kurz, "Ultrahigh-quality-factor silicon-on-insulator microring resonator," Opt. Lett. **29**, 2861-2863 (2004).
5. Q. Xu, B. Schmidt, S. Pradhan, and M. Lipson, "Micrometer-scale silicon electro-optic modulator," Nature **435**, 325-327 (2005).
6. Q. Xu, B. Schmidt, J. Shakya, and M. Lipson, "Cascaded silicon micro-ring modulators for WDM optical interconnection," Opt. Express **14**, 9431-9435 (2006).
7. B. E. Little, J. S. Foresi, G. Steinmeyer, E. R. Thoen, S. T. Chu, H. A. Haus, E. P. Ippen, L. C. Kimerling, and W. Greene, "Ultra-compact Si-SiO2 microring resonator optical channel dropping filters," IEEE Photon. Technol. Lett. **10**, 549-551 (1998).
8. M. A. Popovíc, T. Barwicz, M. R. Watts, P. T. Rakich, L. Socci, E. P. Ippen, F. X. Kärtner, and H. I. Smith, "Multistage high-order microring-resonator add-drop filters," Opt. Lett. **31**, 2571-2573 (2006).
9. S. Xiao, M. H. Khan, S. Shen and M. Qi, "Silicon-on-insulator microring add-drop filters with free spectral ranges over 30 nm," submitted, IEEE J. Lightwave Technol.
10. A. Vörckel, M. Mönster, W. Henschel, P. H. Bolivar, and H. Kurz, "Asymmetrically coupled silicon-on-insulator microring resonators for compact add-drop mutiplexers," IEEE Photon. Technol. Lett. **15**, 921-923 (2003).
11. P. Dumon, W. Bogaerts, V. Wiaux, J. Wouters, S. Beckx, J. V. Campenhout, D. Taillaert, B. Luyssaert, P. Bienstman, D. V. Thourhout, and R. Baets, "Low loss SOI photonic wires and ring resonators fabricated with deep UV lithography," IEEE Photon. Technol. Lett. **16**, 1328-1330 (2004).

#83230 - $15.00 USD Received 18 May 2007; revised 1 Aug 2007; accepted 2 Aug 2007; published 6 Aug 2007

12. V. Van, P. P. Absil, J. V. Hryniewicz and P. –T. Ho, "Propagation loss in single-mode GaAs-AlGaAs microring resonators: measurement and model," IEEE J. Lightwave Technol. **19**, 1734-1739, (2001).
13. R. Grover, V. Van, T. A. Ibrahim, P. P. Absil, L. C. Calhoun, F. G. Johnson, J. V. Hryniewicz, and P. –T. Ho, "Parallel-cascaded semiconductor microring resonators for high-order and wide-FSR filters," IEEE J. Lightwave Technol. **20**, 900-905, (2002).
14. D. Rafizadeh, J. P. Zhang, R. C. Tiberio, and S. T. Ho, "Propagation loss measurements in semiconductor microcavity ring and disk resonators," IEEE J. Lightwave Technol. **16**, 1308-1314, (1998).
15. S. Zhen, H. Chen, and A. W. Poon, "Microring-resonator cross-connect filters in silicon nitride: rib waveguide dimension dependence," IEEE J. Sel. Top. Quantum Electron. **12**, 1380-1387, (2006).
16. B. E. Little, et al, "Microring resonator channel dropping filters," IEEE J. Lightwave Technol. **15**, 998-1005 (1997).

1. Introduction

The high-index-contrast (HIC) in silicon-on-insulator (SOI) strip waveguides allows small bending radii, leading to compact resonators and enabling high-density integration of micro-photonic devices. Accurate quantification of losses in submicrometer-scale SOI waveguides and bends are important for the design and performance of silicon photonic devices, and have gained extensive interests recently [1-3]. Summarized in [3], previously reported methods to measure losses in silicon strip waveguides and bends mainly include cut-back and Fabry-Pérot. Unfortunately, these methods are subject to two major practical limitations: the coupling between the fiber tip and the silicon waveguide as well as silicon waveguide end facets, both of which vary from one waveguide to another. Moreover, such fiber-to-waveguide coupling losses can be much higher than losses in waveguides and bends, leading to high uncertainties in loss measurements. In straight waveguides, the loss is dominated by scattering via sidewall roughness. In 90° or 180° bends, there are two additional sources of loss: bending loss and mode-mismatch loss at the junctions between bending waveguides and straight ones. As losses in SOI bends with large bending radii ($\geq \sim 5$ μm) are rather small, the number of bends required for a measurable total loss is large. Here, we propose and demonstrate a method to characterize losses in bends based on responses of bend-formed racetrack micro-resonators that consist of either two 180° bends or four 90° bends, where straight sections are much shorter than bending sections. We point out that symmetrically coupled add-drop micro-resonators offer a straightforward way to obtain a deterministic estimate of intrinsic losses, and the results are independent of losses associated with fiber coupling in/out or waveguide cleavage facets. The authors in reference [4] reported a fitting method that does not yield deterministic result of losses in SOI resonators. To the best of our knowledge, there has been no reported deterministic and unified analysis of losses in SOI bends and micro-resonators, which is of great importance for building high-performance, highly integrated optical devices based on SOI micro-resonators [5-11].

In this paper, we present a detailed investigation of intrinsic losses in SOI micro-resonators. First, we derive analytical results using the traveling wave theory for the resonator. Losses in resonators are solved with three resonance parameters, *i.e.*, the free spectral range, the minimum transmission of through-port and the -3dB bandwidth of drop-port response. Loss related performance parameters, *e.g.*, the quality-factor and the finesse can also be calculated. As many devices, such as add-drop filters, are symmetrically coupled, our method can extract loss parameters from the device's response itself, without extra fabrication of critically coupled resonators, which can be slightly different with the device itself. Compared to similar investigation of losses in compound semiconductor micro-resonators [12-14] or silicon nitride micro-resonators with rib waveguide [15], our effort is focused on highly compact SOI micro-resonators, and we believe that the new theoretical and experimental approach we demonstrate here can also be applied to resonators fabricated with other materials.

Experimentally, we focused on two symmetrically coupled add-drop racetrack micro-resonators. One resonator has a bending radius of 4.5 μm and a straight section of $\pi/2$ μm,

#83230 - $15.00 USD Received 18 May 2007; revised 1 Aug 2007; accepted 2 Aug 2007; published 6 Aug 2007

and the other one has a bending radius of 2.25 μm and a straight section of π/4 μm. The large difference in the radii of the two resonators leads to significantly different losses in 180° bends. We analyzed detailed performance parameters in these add-drop micro-resonators for a very large wavelength range from ~ 1520 nm to ~ 1630 nm (C and L bands). The propagation loss in a 180° bend is estimated as half of intrinsic losses in a racetrack micro-resonator with very short straight sections.

2. Theories

Our approach is based on the resonance response of a micro-resonator, which is sketched in Fig. 1(a). With the developed traveling wave theory for micro-resonators in [16], we present some new analysis that will be used to characterize losses in micro-resonators. In Fig. 1(a), κ_e^2 and κ_d^2 are the fraction of optical power that the input waveguide and the drop waveguide couple into or out of the micro-resonator respectively. κ_p^2 is the fraction of intrinsic power losses (such as bending, absorption and surface scattering due to roughness) per round-trip in the micro-resonator, and R is the average bending radius of a ring resonator. The intrinsic losses are calculated by $-10\times log_{10}(1-\kappa_p^2)$ dB/round-trip. Figure 1(b) shows sketched power transmission responses of the micro-resonator, where the drop-port response is normalized to the through-port response. The minimum power transmission in the through-port is γ_t at the resonance wavelength λ_o. The through-port extinction is $-10\times log_{10}(\gamma_t)$ in dB. The maximum power transmission on the drop-port is γ_d at the resonance wavelength λ_o. The channel drop loss is $-10\times log_{10}(\gamma_d)$ in dB. The add-drop cross-talk is $-10\times log_{10}(\gamma_d/\gamma_t)$ in dB.

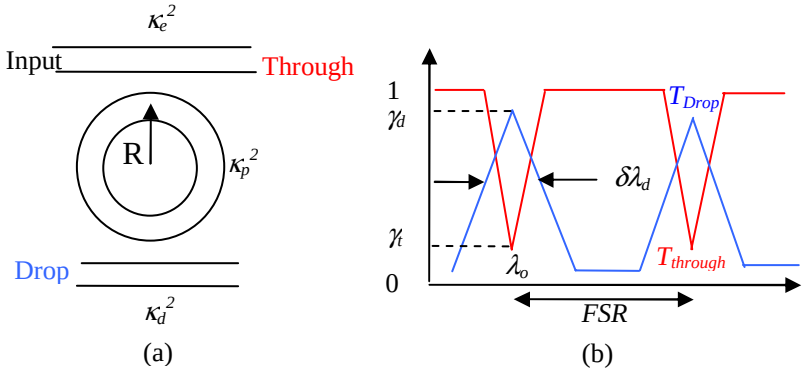

Fig. 1. Theoretical model (a) and schematic power responses (b) of a micro-resonator

In wavelength domain shown in Fig. 1(b), close to each resonance, responses of the through-port and the drop-port can be written as:

$$T_{through} = \frac{(\lambda-\lambda_o)^2 + \left(\frac{FSR}{4\pi}\right)^2 \left(\kappa_d^{\,2} + \kappa_p^{\,2} - \kappa_e^{\,2}\right)^2}{(\lambda-\lambda_o)^2 + \left(\frac{FSR}{4\pi}\right)^2 \left(\kappa_d^{\,2} + \kappa_p^{\,2} + \kappa_e^{\,2}\right)^2} \tag{1.a}$$

$$T_{drop} = \frac{4\times\left(\frac{FSR}{4\pi}\right)^2 \left(\kappa_d^{\,2}\times\kappa_e^{\,2}\right)}{(\lambda-\lambda_o)^2 + \left(\frac{FSR}{4\pi}\right)^2 \left(\kappa_d^{\,2} + \kappa_p^{\,2} + \kappa_e^{\,2}\right)^2} \tag{1.b}$$

#83230 - $15.00 USD Received 18 May 2007; revised 1 Aug 2007; accepted 2 Aug 2007; published 6 Aug 2007

where, $T_{through}$ and T_{drop} are the power transmission of the through-port and the drop-port respectively, and $FSR \approx \lambda^2/(2\pi R n_g)$ is the free spectral range (in wavelength span) in the resonator, and n_g is the group index of lightwave in the micro-resonator. According to Eq. (1.b), the -3dB bandwidth ($\delta\lambda_d$) of the drop-port is related to parameters of waveguide coupling and intrinsic losses by

$$\left(\frac{FSR}{2\pi}\right)\times(\kappa_e^{\ 2}+\kappa_d^{\ 2}+\kappa_p^{\ 2})=\delta\lambda_d \tag{2}$$

Equations (1.a) and (1.b) are mathematically equivalent to previously reported analytical responses of resonators [12-14] with the approximation of near resonance. However, our results have a very simple form in wavelength domain and can be easily understood and compared with measured response, especially in the following scenarios.

Two popular cases of micro-resonators related to applications are discussed here. The first case is micro-resonators without the drop waveguide, *i.e.*, $\kappa_d^2 = 0$. This is a very simple design of microring resonator for applications in recently reported high-quality-factor resonator for sensing applications [4] and microring modulator [5-6]. In this case, the experimental data can be fitted with theoretical through-port transmission in Eq. (1.a). As $T_{through}$ is invariant to the commutation of κ_e^2 and κ_p^2, the larger solution was always conservatively estimated as the upper bound of intrinsic loss [4]. On the other hand, κ_e^2 may also be simulated with the finite-difference time-domain (FDTD) method, so κ_p^2 and κ_e^2 may be determined uniquely assuming a fairly accurate FDTD simulation.

The second case is symmetrically coupled add-drop micro-resonator, *i.e.*, $\kappa_e^2 = \kappa_d^2$, which has been widely used in recent reports of optical add-drop filters [7-11]. By substituting Eq. (2) into Eq. (1.a), noticing $\kappa_e^2 = \kappa_d^2$, we can get

$$T_{through}=\frac{(\lambda-\lambda_o)^2+\left(\frac{FSR}{4\pi}\right)^2\left(\kappa_p^{\ 2}\right)^2}{(\lambda-\lambda_o)^2+\left(\frac{\delta\lambda_d}{2}\right)^2} \tag{3}$$

Noticing $T_{through} = \gamma_t$ for $\lambda = \lambda_o$, we obtain

$$\kappa_p^{\ 2}=2\pi\times\delta\lambda_d\sqrt{\gamma_t}\,/FSR \tag{4}$$

According to Eqs. (2) and (4), the waveguide power coupling coefficients are written as

$$\kappa_e^{\ 2}=\kappa_d^{\ 2}=\pi\times\delta\lambda_d\left(1-\sqrt{\gamma_t}\right)/FSR \tag{5}$$

Thus, in contrast to the first case, the second case gives a deterministic result. Finally, by substituting κ_p^2, κ_e^2 and κ_d^2 into Eq. (1), we can plot the responses to compare with the experimental data, and an excellent match is expected to ensure the validity of our analytical Eqs. (1.a) and (1.b). The merit of our proposed method is its deterministic nature in solving intrinsic losses in resonators, which is independent from losses associated with fiber coupling in/out or waveguide cleavage facets. To our best knowledge, this is in contrast to all previously reported work using fitting methods.

For add-drop micro-resonators, the total quality-factor and the intrinsic quality-factor are defined as $Q_t=\lambda_o/\delta\lambda_d=(2\pi\lambda_o)/[FSR\times(\kappa_e^2+\kappa_d^2+\kappa_p^2)]$ and $Q_i=(2\pi\lambda_o)/(FSR\times\kappa_p^2)=(\lambda_o)/[(\delta\lambda_d)\times(\gamma_t)^{1/2}]$ respectively. The intrinsic quality-factor gives an upper bound of the quality-factor that can be measured in micro-resonators, *i.e.*, $Q_t \le Q_i$. The total finesse and the intrinsic finesse are defined by $F_t = FSR/\delta\lambda_d = 2\pi/(\kappa_e^2+\kappa_d^2+\kappa_p^2)$ and F_i

#83230 - $15.00 USD Received 18 May 2007; revised 1 Aug 2007; accepted 2 Aug 2007; published 6 Aug 2007

$=2\pi/(\kappa_p^2)$ respectively, and naturally $F_t \leq F_i$. For an isolated resonator with a finite initial light power, the intrinsic photon lifetime is defined by the duration for light traveling in the resonator when the light power decays to $1/e^2$. With this definition, the intrinsic photon lifetime in resonators is calculated by $-4\pi R/\ln(1-\kappa_p^2)/v_g = -4\pi n_g R/\ln(1-\kappa_p^2)/c = 2\lambda^2/\ln(1-\kappa_l^2)/c/FSR$. Another important performance parameter of add-drop resonators is the drop-port maximum transmission $\gamma_d=4\times\kappa_e^2\times\kappa_d^2/(\kappa_e^2 + \kappa_d^2 + \kappa_p^2)^2$ according to Eq. (1.b). The theoretical drop loss can be expressed by $-10\times\log_{10}(\gamma_d)=-10\times\log_{10}[4\times\kappa_e^2\times\kappa_d^2/(\kappa_e^2 + \kappa_d^2 + \kappa_l^2)^2]$ in dB. As the intrinsic losses always exist in any real devices, *i.e.*, $\kappa_p^2 > 0$, γ_d is always less than 100%. On the other hand, $\gamma_d \approx 100\%$ if $\kappa_d^2 = \kappa_e^2 \gg \kappa_p^2$ holds, and we also obtain a very high through-port extinction (a low add-drop crosstalk).

In order to estimate the propagation loss in a 180° or 90° bend, we configure racetrack micro-resonators as they are sketched in Figs. 2(a)-2(b). Master Eqs. (1.a) and (1.b) still hold as it is only determined by parameters (*FSR*, κ_d^2, κ_e^2 and κ_p^2) that are independent of the shape of resonators. This means that our discussions above are still valid for resonators sketched in Figs. 2(a)-2(b). If the straight section is much shorter than the bend, *i.e.*, $L \ll \pi R$, intrinsic losses in the micro-resonator are determined by propagation loss in bends, which include the transition loss between the bend and the straight waveguide and intrinsic losses in bending waveguides. In Fig. 2(a), the propagation loss in a 180° bend is half of intrinsic losses in the resonator, *i.e.*, $-5\times\log_{10}(1-\kappa_p^2)$ dB/turn. In Fig. 2(b), the propagation loss in a 90° bend is one quarter of intrinsic losses in the resonator, *i.e.*, $-2.5\times\log_{10}(1-\kappa_p^2)$ dB/turn. Compared to previous reports to measure the propagation loss in bends [3], our method provides a simple and accurate measurement, which is independent of cleaved waveguide facets and the coupling between a fiber tip and the silicon waveguide. In principle, our method does not need to be averaged over multiple measurements, and it can measure low propagation losses in bends with large bending radii without the need to fabricate many bends in a single waveguide.

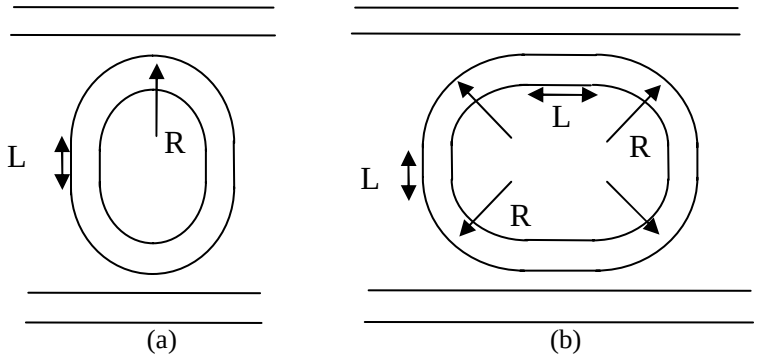

Fig. 2. Generalized racetrack resonator for the estimation of losses in 180° and 90° bends. For an accurate estimation, $L \ll \pi R$ should hold.

3. Experiments

To demonstrate our proposed method experimentally, we focused on racetrack micro-resonators shown in Fig. 2 (a) with two quite different bending radii (4.5 μm and 2.25 μm) for a large contrast of intrinsic losses. Figure 3 presents the scanning-electron micrographs of fabricated micro-resonators. In Fig. 3(a), the micro-resonator has a perimeter of 10π μm, where the bend has a bending radius of 4.5 μm, and each straight section is π/2 μm long. The perimeter of the micro-resonator is linearly scaled down by half in Fig. 3(b) with a much stronger bending radius of 2.25 μm. The fabricated silicon waveguide core has a cross-section of ~ 500 nm × 250 nm supporting the lowest TE mode for wavelengths from 1.52 μm

#83230 - $15.00 USD Received 18 May 2007; revised 1 Aug 2007; accepted 2 Aug 2007; published 6 Aug 2007

to 1.63 μm, the lowest TM mode and higher order modes have much higher propagation losses in waveguides and resonating at different wavelengths due to the strong polarization dependence in silicon waveguides. All waveguide coupling gaps are the same in design, and the calibrated value is 200±10 nm for fabricated devices and different effective indices. Our devices were fabricated in silicon-on-insulator (SOI) wafer (from SOITEC). The top silicon layer thickness is 250 nm and the buried oxide is 3 μm thick. The device patterns were exposed in a 200 nm-thick hydrogen silsesquioxane (HSQ) with the Vistec (formerly Leica) 100 kV electron-beam lithography system installed in the Birck Nanotechnology Center at Purdue University. We used a beam step of 2 nm and an exposure field size of 0.5 mm× 0.5 mm. Inductively-coupled-plasma (ICP) reactive-ion-etch (RIE) with a mixture of Cl_2 and Ar at a pressure of 5 mTorr was applied to etch through the 250 nm silicon layer. As the HSQ (a type of spin-on-glass) is of low loss and has a refractive index of ~ 1.4 at 1.55 μm band, it is not removed after etch but kept intact as a cladding layer.

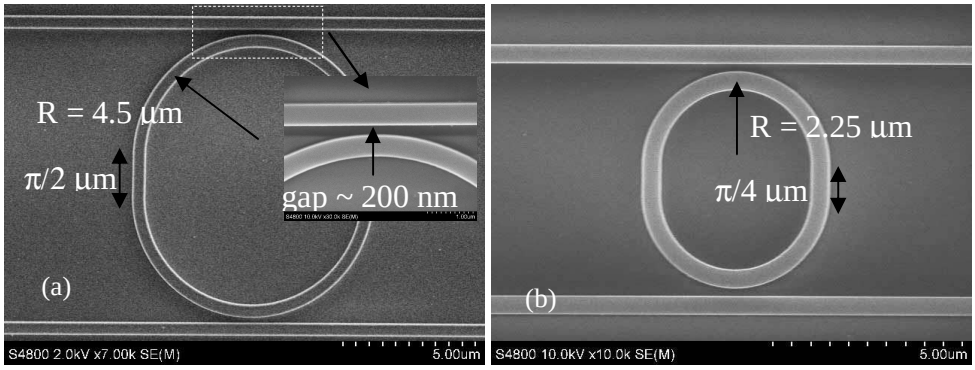

Fig. 3. (a)-(b). Scanning electron micrographs of two fabricated add-drop micro-resonator.

The responses of micro-resonators were characterized by a tunable laser source with wavelengths from 1520 to 1630 nm. Tab. 1 and Tab. 2 list all measured resonance wavelengths for the larger resonators and the smaller resonators, respectively. At each resonance wavelength, three parameters marked in blue color were obtained from measured optical responses, which are the free spectral range (*FSR*), the through-port extinction in dB (related to γ_t) and the drop-port -3dB bandwidth $\delta\lambda_d$. The *FSR* is wavelength dependent over a large wavelength band. So we take the average of two *FSRs* prior to and after a resonance wavelength. κ_p^2, κ_e^2 and κ_d^2 are calculated with Eqs. (4) and (5). Both intrinsic losses in the resonator and the propagation loss in a 180° bend were calculated and highlighted with red color. Performance parameters such as the quality-factor and the finesse were also calculated. For example, at λ ~ 1550 nm, intrinsic losses in the large resonator are 0.14 dB/round-trip, corresponding to an intrinsic quality-factor of Q_i ~ 20,000. Meanwhile, the small resonator has intrinsic losses of 1.23 dB/round-trip, corresponding to an intrinsic quality-factor of Q_i ~ 1200. In the last two rows of each table, we also put the experimental (exp.) channel-drop loss and the theoretical (the.) channel-drop loss. Since the measured channel-drop loss is dependent on cleaved waveguide facets as well as the output coupling between the fiber tip and the waveguide, some discrepancies (~ 1dB) between experimental drop losses and theoretical ones were observed in our case. Please note that the discrepancy may be much larger if the alignment between fiber and waveguide was not optimized well. If the two output waveguides (through and drop) have different propagation losses, this will cause further uncertainty of the exacted channel-drop loss at the resonator. A large error of channel-drop loss may cause errors in the fitting method used in [12-15], while our proposed method will not be affected. In addition, we also fabricated and characterized the generalized

#83230 - $15.00 USD Received 18 May 2007; revised 1 Aug 2007; accepted 2 Aug 2007; published 6 Aug 2007

racetrack resonator (R = 4.5 μm) shown in Fig. 2(b), and the intrinsic losses at 1.55 μm is 0.26 dB/round-trip, which are indeed almost doubled compared to the racetrack resonator shown in Fig. 2(a). For a 90° bend, the propagation loss is 0.06 dB/turn at 1.55 μm.

Table 1 Loss parameters for the large micro-resonator shown in Fig. 3(a)

Resonance Wavelength (nm)	1522.16	1537.90	1554.00	1570.65	1587.81	1605.56	1623.91
FSR (nm)	15.74	15.92	16.38	16.91	17.45	18.05	18.35
Exp. Extinction -10×log10(γ_t) dB	16.87	17.61	17.69	19.38	20.49	19.61	19.43
Exp. Bandwidth $\delta\lambda_d$ (nm)	0.45	0.50	0.65	0.80	0.95	1.15	1.40
κ_p^2	0.0257	0.026	0.0325	0.032	0.0323	0.0418	0.0512
$\kappa_d^2 = \kappa_e^2$	0.077	0.0857	0.1085	0.1327	0.1549	0.1792	0.214
Intrinsic losses (dB/round-trip)	0.11	0.11	0.14	0.14	0.14	0.185	0.228
Losses in a 180° Bend (R = 4.5 μm)	0.055	0.055	0.07	0.07	0.07	0.0925	0.114
Total Q	3383	3076	2391	1963	1671	1396	1160
Intrinsic Q	23643	23345	18347	18243	17700	13374	10860
Total F	35	32	25	21	18	16	13
Intrinsic F	244	242	193	196	195	150	123
Exp. Drop loss (dB)	2.14	0.66	0.55	0.47	0.01	0.30	≈ 0
The. Drop loss (dB)	1.34	1.23	1.21	0.99	0.86	0.96	0.98

Table.2 Loss parameters for the small micro-resonator shown in Fig. 3(b)

Resonance Wavelength (nm)	1524.2	1555.4	1588.3	1623.7
FSR (nm)	31.2	32.1	34.2	35.4
Exp. Extinction (dB) -10×log10(γ_t) dB	3.5	4.0	5.0	6.0
Bandwidth (nm) $\delta\lambda_d$ (nm)	1.9	2.0	2.2	2.9
κ_p^2	0.2557	0.2474	0.2276	0.258
$\kappa_d^2 = \kappa_e^2$	0.0634	0.0723	0.0886	0.1284
Intrinsic losses (dB/round-trip)	1.28	1.23	1.12	1.29
Losses in a 180° bend (R=2.25 μm)	0.64	0.62	0.56	0.65
Total Q	802	778	722	560
Intrinsic Q	1200	1233	1284	1117
Total F	16.4	16.0	15.5	12.2
Intrinsic F	24.6	25.4	27.6	24.4
Exp. Drop loss (dB)	13.0	10.0	8.0	6.0
The. Drop loss (dB)	9.6	8.7	7.2	6.0

#83230 - $15.00 USD Received 18 May 2007; revised 1 Aug 2007; accepted 2 Aug 2007; published 6 Aug 2007

Most recently, we achieved intrinsic quality-factors of Q_i ~ 6,000 (κ_p^2 ~ 0.05, or 0.22 dB/round-trip) and Q_i ~ 100,000 (κ_p^2 ~ 0.005, or 0.022 dB/round-trip) at resonance wavelengths close to 1550 nm in microring resonators with R=2.25 μm and R=4.5 μm respectively. These intrinsic quality-factors are as large as five times of those in racetrack resonators with the same bending radius. Therefore the transition loss between the bend and the straight waveguide is a major source of intrinsic losses in racetrack resonators. It can even dominate other loss mechanisms in the small racetrack resonator (R=2.25 μm). This is supported by the fact that the small racetrack resonator shows approximately constant intrinsic losses of ~ 1.2 dB/round-trip for wavelengths from 1520 to 1630 nm. Normally, more optical power distributes outside of the waveguide core at longer wavelengths, so the bending loss and the surface-roughness scattering loss increase. This is the case in the large racetrack resonator (R=4.5 μm), where intrinsic losses increase from 0.11 dB to 0.23 dB per round-trip for wavelengths from 1520 to 1630 nm.

With extracted parameters κ_p^2, κ_d^2 and κ_e^2 in Tab. 1 at two center resonance wavelengths of ~ 1522 nm and ~ 1554 nm, we plot in Fig. 4 theoretical response curves and compare them with experiments. The red ($T_{through}$) and green (T_{drop}) curves are plotted according to Eqs. (1.a) and (1.b) respectively, and blue dots and black dots represent measured responses of through-port and drop-port respectively. The wavelength scan step is 0.01 nm for the measurements. In addition to small background noise fluctuations, the ripples of experimental responses are mainly due to the Fabry-Pérot effect in silicon waveguides with ~ 5 mm length, which is inevitable when coupling the light into and out of the micro-resonator. Generally, the experimental responses match well with the theoretical curves.

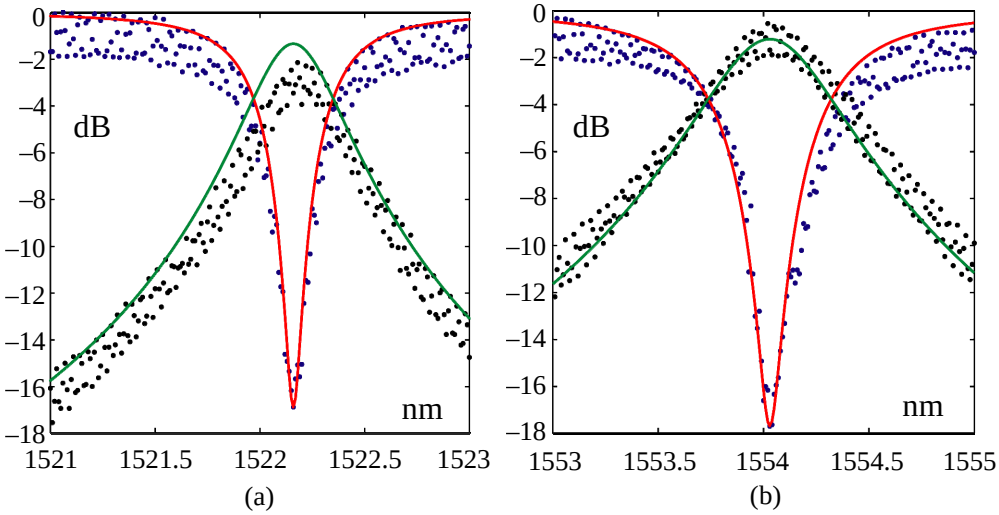

Fig. 4. Comparison of theoretical (red and green lines) and measured (blue and black dots) responses of resonators at two wavelengths.

Finally, we discuss the accuracy of our calculated κ_p^2 or intrinsic quality-factor. The first error source is possibly the slight asymmetry due to fabrication imperfection, *i.e.*, κ_e^2 differs by a very small amount from κ_d^2. If such a difference between κ_e^2 and κ_d^2 is larger than κ_p^2, it is then difficult to give an accurate estimation of κ_p^2 with our proposed method. Although the asymmetry can be significantly reduced by high-quality nanofabrication, this problem in fact

#83230 - $15.00 USD Received 18 May 2007; revised 1 Aug 2007; accepted 2 Aug 2007; published 6 Aug 2007

may be solved with weakly coupled resonators, *i.e.*, increasing the coupling gap to reduce waveguide power coupling. For example, for a very high intrinsic quality-factor over 200,000, κ_p^2 is less than ~ 0.25%, and weakly coupled resonator should be adopted, *e.g.*, $\kappa_d^2=\kappa_e^2 \sim \kappa_p^2$. As a specific case, the intrinsic quality-factor can be estimated approximately with the total quality-factor if $\kappa_d^2=\kappa_e^2 \ll \kappa_p^2$ in weakly coupled resonators, *i.e.*, $Q_t=\lambda_o/\delta\lambda_d=(2\pi\lambda_o)/[FSR\times(\kappa_e^2+\kappa_d^2+\kappa_p^2)]\approx(2\pi\lambda_o)/[FSR\times\kappa_p^2]=Q_i$. The second error source is from experiments. According to $\kappa_p^2=2\pi\times(\delta\lambda_d)\times(\gamma)^{1/2}/FSR$ and $Q_i=(2\pi\lambda_o)/(FSR\times\kappa_p^2)=(\lambda_o)/((\delta\lambda_d)\times(\gamma)^{1/2})$, the relative errors of κ_p^2 and Q_i can be expressed by

$$\left|\frac{\Delta\left(\kappa_p^{\,2}\right)}{\kappa_p^{\,2}}\right| = \left|\frac{\Delta(\delta\lambda_d)}{\delta\lambda_d}+\frac{\Delta\left(\gamma_t^{\,1/2}\right)}{\gamma_t^{\,1/2}}-\frac{\Delta(FSR)}{FSR}\right| \le \left|\frac{\Delta(\delta\lambda_d)}{\delta\lambda_d}\right|+\left|\frac{\Delta\left(\gamma_t^{\,1/2}\right)}{\gamma_t^{\,1/2}}\right|+\left|\frac{\Delta(FSR)}{FSR}\right| \quad (6.a)$$

$$\left|\frac{\Delta Q_i}{Q_i}\right| = \left|\frac{\Delta(\delta\lambda_d)}{\delta\lambda_d}+\frac{\Delta\left(\gamma_t^{\,1/2}\right)}{\gamma_t^{\,1/2}}\right| \le \left|\frac{\Delta(\delta\lambda_d)}{\delta\lambda_d}\right|+\left|\frac{\Delta\left(\gamma_t^{\,1/2}\right)}{\gamma_t^{\,1/2}}\right| \quad (6.b)$$

For the data in Tab. 1, the relative error of *FSR* is trivial (only ~ 0.01/16 due to the laser wavelength scanning step of 0.01 nm). For a rough estimation, due to the potential background noise and the Fabry-Pérot effect, the relative error of $\delta\lambda_d$ is within ±5% for ±0.025 nm error in measured bandwidth, and the relative error of $(\gamma)^{1/2}$ is within ±5% for ±0.5 dB error in measured extinction of ~ 20 dB. Thus, the relative error of intrinsic quality-factor is ±10%. To have a more accurate estimate, the Fabry-Pérot effect should be suppressed to reduce data fluctuation.

4. Conclusion

In conclusion, we have demonstrated a new method to characterize intrinsic losses in micro-resonators. We designed and presented two cases to retrieve intrinsic losses. The first case is for micro-resonators with only the input/through waveguide. The second case, which yields deterministic results, is for micro-resonators in a symmetrically coupled add-drop configuration. For symmetrically coupled add-drop micro-resonators, by extracting the free spectral range, the through-port extinction and the drop -3dB bandwidth at resonance, intrinsic losses and intrinsic quality-factor can be calculated. Our approach to measure intrinsic losses in resonators provides a novel way to measure losses in 180° bends or 90° bends. We characterized losses in fabricated SOI resonators. At 1.55 μm, racetrack resonators with a bending radius of 4.5 μm show intrinsic losses as small as 0.14±0.014 dB/round-trip. Meanwhile, intrinsic losses increase up to 1.23 dB/round-trip in the resonator that has a bending radius of 2.25 μm. Losses in a 180° bend are estimated as a half of the intrinsic losses in these racetrack resonators, *i.e.*, 0.07±0.007 dB/turn for a bending radius of 4.5 μm and 0.62 dB/turn for a bending radius of 2.25 μm. Loss in a 90° bend with a radius of 4.5 μm is determined to be 0.06±0.006 dB/turn at 1.55 μm. Compared to the well-known cut-back method to measure losses in these bends, our scheme has notable merits including much lower complexity in fabrication (much reduced number of bends required) and much higher accuracy for low-loss bends with large bending radii in principle. The accuracy in our calculation of intrinsic quality-factor in micro-resonators is also discussed, and is believed to be limited by the Fabry-Pérot effect in our measurements. However, it is not a fundamental limit for our method.

#83230 - $15.00 USD Received 18 May 2007; revised 1 Aug 2007; accepted 2 Aug 2007; published 6 Aug 2007